UvA-DARE (Digital Academic Repository)

Resonance-enhanced multiphoton ionization photoelectron spectroscopy of even-parity autoionizing Rydberg states of atomic sulphur

Woutersen, S.; de Milan, J.B.; de Lange, C.A.; Buma, W.J.

Link to publication

Resonance-enhanced multiphoton-ionization photoelectron spectroscopy of even-parity autoionizing Rydberg states of atomic sulphur

S. Woutersen,[a] J. B. Milan, W. J. Buma, and C. A. de Lange
Laboratory for Physical Chemistry, University of Amsterdam, Nieuwe Achtergracht 127, 1018 WS Amsterdam, The Netherlands

Several previously unobserved Rydberg states of the sulphur atom above the lowest ionization threshold are identified and assigned using $(2+1)$ resonance-enhanced multiphoton-ionization photoelectron spectroscopy. All states were accessed by two-photon transitions from either the ^3P ground or the ^1D excited state, prepared by *in situ* photodissociation of H_2S. The observed states derive from the $(^2D^o)5p$ and $(^2P^o)4p$ configurations. For the $(^2D^o)5p\ ^3F$ and $(^2P^o)4p\ ^3D$ triplets, extensive photoelectron spectroscopic studies enable a detailed comparison of the autoionization and photoionization rates of these states. © *1997 American Institute of Physics.* [S0021-9606(97)01317-2]

I. INTRODUCTION

A detailed knowledge of the energy levels, oscillator strengths, and photoionization cross sections of the S atom is of fundamental interest for understanding the spectroscopy and dynamics of open-shell atoms,[1] and is of astrophysical relevance because of the high abundance of sulphur in the interstellar medium and in the sun.[2] Even-and odd-parity excited states of the atom have been extensively investigated by one-photon vacuum ultraviolet absorption[3–5] and photoionization[6] studies, and by $(2+1)$ resonance enhanced multiphoton ionization (REMPI) spectroscopy.[7–11] Recently we reported on a $(2+1)$ REMPI-photoelectron spectroscopy (REMPI-PES) study of the S atom, in which Rydberg states converging upon the lowest ionic state were investigated.[12] In this study, some 20 hitherto unobserved even-parity Rydberg states belonging to the $(^4S^o)nf\ ^3F$ and $(^4S^o)np\ ^3P$ series have been characterized. Photoelectron spectroscopy and analysis of the quantum defects of the latter series clearly showed that it is perturbed around $n=7$ by the $(^2D^o)4p\ ^3P$ interloper state. Moreover, the extensive observation of the $(^4S^o)np\ ^3P$ series enabled the lowest ionization energy to be determined with improved accuracy as 83560.8 ± 0.1 cm^{-1}.

In the present study we shall be concerned with Rydberg states converging upon excited ionic states, and located in the energy region above the lowest ionization threshold. Here, new states have been observed that derive from the $(^2D^o)5p$ and $(^2P^o)4p$ configurations, and which include the $(^2D^o)5p\ ^3F$ and $(^2P^o)4p\ ^3D$ states, accessed from the ^3P ground state. These states can decay into the $^4S^o$ continua, and as it turns out, the autoionization rates are small enough that at sufficient laser intensities, photoionization into the $^2D^o$ and $^2P^o$ continua will compete with autoionization. The observed ionic state branching ratios then reflect the relative magnitudes of the one-photon absorption and autoionization rates of these excited states. Apart from the transitions to the

$(^2D^o)5p\ ^3F$ and $(^2P^o)4p\ ^3D$ states, the excitation spectra show resonance enhancement as well from several other states deriving from the $(^2D^o)5p$ and $(^2P^o)4p$ configurations. Combination of photoelectron spectra obtained for ionization *via* these levels and the relative transition intensities leads to assignments of these states.

II. EXPERIMENTAL DETAILS

The experimental setup has been described elsewhere.[13] In short, the frequency-doubled output of an excimer pumped dye laser is focused into the ionization chamber of a ''magnetic bottle'' electron spectrometer. With this electron spectrometer, REMPI spectroscopy is performed using either kinetic energy-resolved photoelectron detection or mass-resolved ion detection.[14]

The dye laser wavelength calibration was performed using two-photon transitions to known states of atomic sulphur and xenon, and resulted in an uncertainty of 0.3 cm^{-1} at the two-photon level in the line positions tabulated in the following.

Two kinds of experiments have been performed. First, excited states were located by scanning the excitation wavelength while simultaneously detecting either the S$^+$ ion signal or the electron current. Secondly, at a given excitation wavelength the photoelectrons were analyzed according to their kinetic energies.

Sulphur atoms are produced *in situ* by subsequent photodissociation of H_2S and HS, which results in the formation of H(^2S) and S(^3P, ^1D).[15] The S($^3P_2$):S($^3P_1$): S($^3P_0$) fine-structure branching ratio for this process has been found to be only slightly colder than the statistical distribution 5:3:1.[15]

In the present study, photodissociation and subsequent REMPI spectroscopy are carried out with one laser only. The concentration of sulphur atoms in the ionization chamber may therefore depend on the excitation wavelength. However, the S concentration is expected to be a slowly varying function of the wavelength, allowing for the comparison of

[a]Present address: FOM-Institute for Atomic and Molecular Physics, Kruislaan 407, 1098 SJ Amsterdam, The Netherlands.

intensities of peaks lying within a limited excitation energy interval.

H_2S (99.6%, Messer Griesheim) is introduced into the ionization chamber using an effusive inlet. Typical operating pressure are 10^{-4} mbar in the ionization chamber and 10^{-6} mbar in the flight tube.

III. RESULTS AND DISCUSSION

A. General considerations

The ground-state electronic configuration of atomic sulphur is $1s^2 2s^2 2p^6 3s^2 3p^4$, which gives rise to the three terms ^3P, ^1D, and ^1S in order of increasing energy. The ^3P ground state is inverted, the $^3P_1$ and $^3P_0$ states lying 369.06 and 573.64 cm^{-1} above the $^3P_2$ state, respectively; the energies of the $^1D_2$ and $^1S_0$ states are 9239.61 and 22 179.95 cm^{-1}.[16] Removal of an outer electron produces the S^+ ion in its lowest electronic configuration, $...3p^3$, giving rise to the $^4S^o$ ground and $^2D^o$ and $^2P^o$ excited ionic states, which lie 83 559.1, 98 428 (mean value), and 108 107 cm^{-1} (mean value) above the S I ground state, respectively.

In the present study, two-photon transitions from the ^3P ground and ^1D excited state have been observed. Strict two-photon selection rules are $|\Delta J| = 0,1,2$ with $J = 0 \leftrightarrow J = 1$ forbidden, and the parity selection rule *odd–odd, even–even*. For $(^2D^o)5p$ and $(^2P^o)4p$ states the principal quantum number is low enough to justify application of the *LS*-coupling scheme. In fact, the $(^2D^o)5p\,^1F_3$ and $(^2D^o)5p\,^3F_{2,3,4}$ states were found to lie ~ 70 cm^{-1} apart, which is reasonably large compared to the spin–orbit splitting of ~ 30 cm^{-1} in the $^2D^o$ ionic core. In the *LS*-scheme the additional two-photon selection rules $\Delta S = 0$ and $|\Delta L| = 0,1,2$ (with $L = 0 \leftrightarrow L = 1$ forbidden) apply.

B. $(^2D^o)5p\,^3F$ and $(^2P^o)4p\,^3D$ autoionizing states

1. Wavelength studies

The two-photon energy region from 83 600 cm^{-1}, just above the lowest ionization energy, up to 89 000 cm^{-1} was scanned employing mass-resolved resolved ion detection, monitoring the S^+ channel. This region contains mostly transitions from the $^1D_2$ excited state to higher members of the $(^2D^o)np$ and $(^2D^o)nf$ Rydberg series, which have been extensively documented.[11] However, in the region from 87 200 to 89 000 cm^{-1}, shown in Fig. 1(a), several intense peaks corresponding to transitions from the ^3P ground state are seen as well. These transitions have not been observed in Ref. 11, since in that experiment atomic sulphur was prepared by photodissociation of OCS, which yields mainly $S(^1D_2)$, and very little $S(^3P)$. Some of the transitions from the ^3P state can in fact be seen as very weak features in the wavelength scans of Ref. 11, but they have not been commented on. Three other broad peaks in these spectra were attributed to transitions from the ^3P state.[11] As these peaks could not be observed in the present experiments, it seems more probable that they derive from molecular resonances.
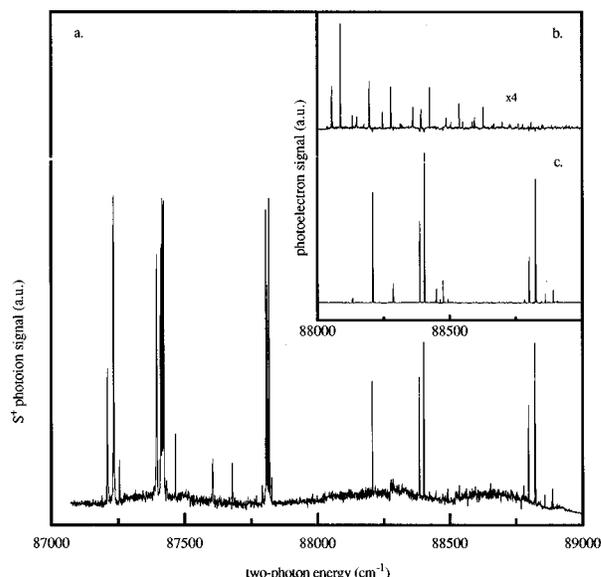

FIG. 1. Wavelength scans (not corrected for dye efficiency) covering the two-photon energy region from 87 000 to 89 000 cm^{-1}. Scan (a) has been recorded employing mass-resolved ion detection, monitoring the S^+ channel. Scans (b) and (c) have been recorded employing kinetic energy-resolved photoelectron detection, monitoring electrons with kinetic energies of 1.8 eV in (b) and with kinetic energies larger than 2.5 eV in (c).

In the two-photon energy region from 88 000 to 89 000 cm^{-1}, the signal-to-noise ratios are rather low when mass-resolved ion detection is used. For this reason, excitation spectra employing kinetic energy-resolved electron detection were recorded as well. The resulting excitation spectra are shown in Figs. 1(b) and (c). When electrons with kinetic energies of 1.8 eV are monitored, transitions from the $^1D_2$ state to the strongly autoionizing $(^2D^o)np$ and $(^2D^o)nf$ Rydberg states reported previously[11] can be reproduced for $n = 10-15$ [see Fig. 1(b)], though our measured transition energies differ systematically by about 1 cm^{-1} from the ones reported in this study. When electrons with kinetic energies larger than 2.5 eV are monitored, the $(2+1)$ REMPI transitions from the ^3P_J ground state are observed [see Fig. 1(c)].

In Fig. 1(a) 13 intense peaks can be distinguished that correspond to transitions from the $^3P_2$, $^3P_1$, and $^3P_0$ ground-state fine-structure levels to two triplet states, which lie 87 820 cm^{-1} and 88 800 cm^{-1} above the $^3P_2$ ground state, respectively. The line positions of these transitions are listed in Table I. The initial state of every transition can be identified by observation of the $^3P_1 - {}^3P_2$, and $^3P_0 - {}^3P_2$ ground-state splittings in the spectrum. The linewidths of the resonances in Fig. 1 are 1.0 cm^{-1}, but can be reduced to 0.6 cm^{-1} when lower laser powers are employed. Since the laser bandwidth and Doppler broadening are responsible for a contribution of ~ 0.6 cm^{-1}, it appears that there is little lifetime broadening, indicating slow autoionization rates.

On the basis of quantum defect considerations, the states in this energy region are expected to have either a $(^2D^o)5p$ or a $(^2P^o)4p$ configuration (at an energy of 88 800 cm^{-1}, the effective quantum number is 3.38 with

TABLE I. Observed transitions from the ground state to autoionizing triplet states. The uncertainty in the wave numbers is estimated to be 0.3 cm^{-1}. In the last three columns the ionic state branching ratios observed by photoelectron spectroscopy for ionization *via* the given levels are reported. Previously unobserved term levels are denoted by asterisks. All photoelectron spectra have been recorded with equal laser intensity.

$2h\nu$ (cm^{-1})	Excited state energy[a] (cm^{-1})	Initial state	Excited state	$^4S^o(\%)$[b]	$^2D^o(\%)$	$^2P^o(\%)$
87 251.1	87 824.7*	$^3P_0$	$(^2P^o)4p\ ^3D_2$	90	1	9
87 428.8	87 824.9*	$^3P_1$	$(^2P^o)4p\ ^3D_2$	87	0	13
87 433.6	87 829.7*	$^3P_1$	$(^2P^o)4p\ ^3D_1$	72	4	24
87 440.2	87 836.3*	$^3P_1$	$(^2P^o)4p\ ^3D_3$	10	8	82
87 824.7	87 824.7*	$^3P_2$	$(^2P^o)4p\ ^3D_2$	89	1	10
87 829.7	87 829.7*	$^3P_2$	$(^2P^o)4p\ ^3D_1$	80	4	16
87 835.9	87 835.9*	$^3P_2$	$(^2P^o)4p\ ^3D_3$	25	7	68
88 226.1	88 799.7[c]	$^3P_0$	$(^2D^o)5p\ ^3F_2$	79	20	1
88 403.6	88 799.7[c]	$^3P_1$	$(^2D^o)5p\ ^3F_2$	72	27	1
88 421.2	88 817.3*	$^3P_1$	$(^2D^o)5p\ ^3F_3$	57	43	0
88 799.6	88 799.6[c]	$^3P_2$	$(^2D^o)5p\ ^3F_2$	87	13	0
88 817.0	88 817.0*	$^3P_2$	$(^2D^o)5p\ ^3F_3$	70	30	0
88 841.2	88 841.2*	$^3P_2$	$(^2D^o)5p\ ^3F_4$	58	42	0

[a]Excited state energy calculated with respect to the $^3P_2$ ground state.
[b]S$^+$($^4S^o$) produced by autoionization of the excited state.
[c]Energy level reported previously[9] to lie at 88 799.2$\pm$2 cm^{-1}.

respect to the $^2D^o$ ionic limit and 2.38 with respect to the $^2P^o$ ionic limit). Photoelectron spectra obtained *via* these resonances (see Table I) unambiguously identify the ionic core as $^2D^o$ for the triplet at approximately 88 800 cm^{-1} and $^2P^o$ for the triplet at approximately 87 820 cm^{-1}.

The $(^2D^o)5p$ triplet may be either a ^3P, ^3D, or ^3F state. The ^3P state, which can couple by electrostatic interaction to the $(^4S^o)\epsilon p\ ^3P$ continua, is expected to be strongly autoionizing, and the accompanying lifetime broadening will probably render this state unobservable by REMPI methods. In fact, in a study of atomic oxygen,[17] the linewidth FWHM of the autoionizing $(^2D^o)3p\ ^3P$ state has been found to be 800 cm^{-1}. The linewidth of the $(^2D^o)5p\ ^3P$ state in atomic sulphur can be expected to be of the same order of magnitude. The observed resonances must therefore be attributed to either a ^3D or ^3F state. The fact that only two fine-structure levels of the triplet are observed to be accessible from the $^3P_1$ ground-state level (see the spectrum at 88 400 cm^{-1} in Fig. 1) strongly suggests that the triplet is ^3F rather than ^3D, since the $^3F_4$ level cannot be reached by a two-photon excitation from the $^3P_1$ level. In contrast, three transitions from the $^3P_1$ level would be expected if the triplet were a ^3D state, since all three of the $^3D_{1,2,3}$ fine-structure levels are accessible from the $^3P_1$ level. Accordingly, the $(^2D^o)5p$ triplet is assigned as ^3F. Using the two-photon selection rules, the ^3F fine-structure levels can be assigned unambiguously. The state at 88 841.2 cm^{-1} must be assigned as the $^3F_4$ fine-structure level, as it is accessible from the $^3P_2$ level, but not from the $^3P_1$ level. Furthermore, the state at 88 799.6 cm^{-1} must be assigned to the $^3F_2$ level, as this is the only ^3F level accessible by two-photon absorption from the $^3P_0$ state. The remaining state at 88 817.0 cm^{-1} must consequently be the $^3F_3$ level. Thus, the $^3F_{2,3,4}$ ordering is the same as for the first series member $(^2D^o)4p\ ^3F$. Furthermore, the fine-structure splitting decreases by a factor

of 0.7, going from $4p$ to $5p$, which is of the order of the expected factor $(4/5)^3 \approx 0.5$.

A detailed scan, shown in Fig. 2(a), was recorded in order to determine the relative line strengths of the fine-structure transitions. These can be compared with theoretical values for a $^3P \rightarrow {}^3F$ two-photon transition, which can be calculated using the spherical tensor formalism described in Refs. 18 and 19. In the LS-approximation, both the Hamiltonian in the absence of the radiation field H_0, and the dipole operator D, commute with the total spin operator S.[20] It can then be shown that for linearly polarized light the relative line strengths $I(J \rightarrow J')$ of a $\gamma LSJ \rightarrow \gamma'L'S'J'$ two-photon transition (where γ stands for all quantum numbers other than L, S, and J) are given by
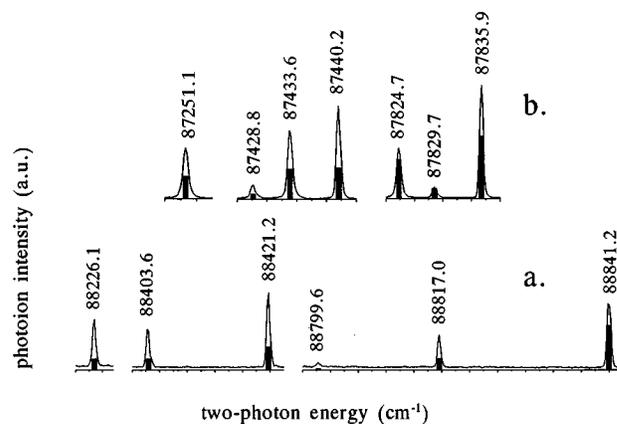

FIG. 2. Detailed wavelength scans recorded employing mass-resolved ion detection, showing the transitions listed in Table I. The three scans of (a) were recorded with equal laser intensity; likewise for (b). The bars represent calculated two-photon line strengths for $^3P \rightarrow {}^3F$ (a) and $^3P \rightarrow {}^3D$ (b) fine-structure transitions (see the text for details).

TABLE II. Calculated relative line strengths for the $^3P_J \rightarrow {}^3F_{J'}$ transition. The values have been normalized w.r.t. the $^3P_1 \rightarrow {}^3F_3$ line strength.

J	J'	$I(J \rightarrow J')$
0	2	0.500
1	2	0.500
1	3	1.000
2	2	0.071
2	3	0.500
2	4	1.928

$$I(J \rightarrow J') = \tfrac{1}{3}(2J'+1)(2J+1)$$

$$\times \begin{Bmatrix} L' & J' & S \\ J & L & 0 \end{Bmatrix}^2 |\langle \gamma'L' \| Q^o \| \gamma L \rangle|^2 \delta_{S'S}$$

$$+ \tfrac{2}{15}(2J'+1)(2J+1)$$

$$\times \begin{Bmatrix} L' & J' & S \\ J & L & 2 \end{Bmatrix}^2 |\langle \gamma'L' \| Q^2 \| \gamma L \rangle|^2 \delta_{S'S}, \quad (1)$$

where the reduced matrix elements $\langle \gamma'L' \| Q^o \| \gamma L \rangle$ and $\langle \gamma'L' \| Q^2 \| \gamma L \rangle$ of the zero- and second-order irreducible tensor operators Q^k are defined in Ref. 18. If $L \neq L'$, the first $6j$-symbol vanishes, and the relative line strengths can be calculated algebraically. The resulting values for a $^3P_J \rightarrow {}^3F_{J'}$ two-photon transition are given in Table II. In Fig. 2(a) they are compared with the experimentally determined line strengths. The scans in this figure were recorded using mass-resolved ion detection, with identical H_2S pressure and laser intensity. In the calculation the $S(^3P_2){:}S(^3P_1){:}S(^3P_0)$ distribution was assumed to be 5:3:1, following Ref. 15. The agreement between the theoretical and experimental line strengths seems to justify the assignments of the ^3F_J fine-structure levels. Closer inspection of Fig. 2(a) suggests that the $S(^3P_2){:}S(^3P_1){:}S(^3P_0)$ distribution deviates slightly from the statistical distribution 5:3:1, showing a preference for $S(^3P_1)$ and $S(^3P_0)$. However, the deviations may also be due to changes in photodissociation cross sections of either SH or H_2S, or to dye gain effects.

The possible $(^2P^o)4p$ triplet states are ^3P and ^3D. The $(^2P^o)4p$ ^3P state will be strongly autoionizing and can probably not be observed for reasons mentioned previously. It therefore seems that the triplet can only be a ^3D state. This assumption is confirmed by the observed transitions. The spectrum shows that only one of the triplet fine-structure levels is accessible from the $^3P_0$ level, which is to be expected for a $^3D_{1,2,3}$ state, since the $J=3$ level cannot be reached from $J=0$, and $J=0 \rightarrow J=1$ two-photon transitions are strictly forbidden. All three of the $^3D_{1,2,3}$ fine-structure levels are accessible from the $^3P_1$ and $^3P_2$ levels, which is in agreement with the two triplet structures observed in the spectrum at 87 430 and 87 830 cm^{-1}. The assignments of the fine-structure levels are given in Table I. The state at 87 824.7 cm^{-1} can immediately be assigned as $^3D_2$, as this is the only level accessible from the $^3P_0$ level. The assignment of the two remaining levels at 87 829.7 and 87 835.9 cm^{-1}, which must be the $^3D_1$ and $^3D_3$ states, is not

possible on the basis of two-photon selection rules. The theoretical values of the relative line strengths of a $^3P_J \rightarrow {}^3D_{J'}$ two-photon transition have been calculated before.[21] Equation (1) reproduces the values given in this previous paper. From these calculated values it follows that the $^3P_2 \rightarrow {}^3D_3$ transition should be 6.2 times stronger than the $^3P_2 \rightarrow {}^3D_1$ transition. Since the resonance at 87 835.9 cm^{-1} is observed to be ~ 8 times stronger than the resonance at 87 829.7 cm^{-1}, it seems justified to assign the state at 87 835.9 cm^{-1} as $^3D_3$ and the state at 87 829.7 cm^{-1} as $^3D_1$. As can be seen in the scan shown in Fig. 2(b), the observed fine-structure line strengths agree reasonably well with the values predicted on the basis of the present assignments.

In a previous REMPI-PES study of atomic sulphur,[7] a resonance at 66 758 cm^{-1} has been attributed to a spin-forbidden $^1S_0 \rightarrow (^2P^o)4p$ $^3D_2$ transition, which would place the $(^2P^o)4p$ $^3D_2$ state at an energy of 88 925 cm^{-1}. The fact that at 79 683.5 cm^{-1} a very strong transition from the $^1D_2$ excited state to the 88 925 cm^{-1} level is observed (see Table III), and that only very weak signals corresponding to transitions from the $^3P_2$ and $^3P_1$ levels can be observed [see Fig. 1(c) and Table III], suggests that this state must rather be assigned as a singlet state, possibly $(^2P^o)4p$ $^1D_2$ (see Sec. C).

It seems that none of the states given in Table I can be accessed from either the $^1D_2$ or the $^1S_0$ excited state, except for the level at 88 799.7 cm^{-1}, which is assigned here as $(^2D^o)5p$ $^3F_2$. In a previous REMPI study of atomic sulphur,[9] a weak two-photon transition from the $^1S_0$ state to this level [which the authors have tentatively assigned as $(^2P^o)4p$ $^3D_2$] has been observed. In addition, in the present study a very weak transition from the $^1D_2$ excited state to the level at 88 799.7 cm^{-1} was observed at a two-photon energy of 79 561.0 cm^{-1} (see Table III). No other transitions from the $^1D_2$ state to any of the levels given in Table I are observed. The fact that such spin-forbidden transitions to the $(^2D^o)5p$ ^3F and $(^2P^o)4p$ ^3D do not occur or are very weak indicates that the LS-coupling scheme may be considered appropriate.

2. Photoelectron studies

Photoelectron spectra have been recorded for all the $^3P \rightarrow {}^3D$ and $^3P \rightarrow {}^3F$ transitions, and the observed ionic state branching ratios are given in Table I. As can be expected, the branching ratios for a given excited state are virtually independent of the initial ^3P fine-structure state from which it is excited.

Apart from photoelectron peaks due to $(2+1)$ REMPI, all the photoelectron spectra show a peak at a photoelectron energy of $2h\nu - 10.36$ eV, which is due to autoionization of the excited state into the $(^4S^o)\epsilon l$ continua. In fact, the two processes compete, and the excited state can either decay by autoionization, leaving the ion in the $^4S^o$ ground state, or absorb another photon and subsequently ionize, leaving the ion in one of the two excited ionic states or the ground ionic state. As the photoionization probability is proportional to the photon flux, the relative branching ratios are expected to

TABLE III. Observed excited state levels and ionic state branching ratios in the energy region 87 000–89 000 cm^{-1} and tentative assignments. Previously unobserved levels are denoted by asterisks.

$2h\nu$ (cm^{-1})	Excited state energy (cm^{-1})[a]	Initial state	Lit. value	$^2D^o$(%)	$^2P^o$(%)	Assignment
78 385.6	87 624.2	$^1D_2$	87 624[b]	12	88	$(^2P^o)4p\ ^1P_1$
79 561.0	88 799.6	$^1D_2$	88 799[c]	81	19	$(^2D^o)5p\ ^3F_2$
79 638.7	88 877.3	$^1D_2$	88 876[d]	68	32	$(^2D^o)5p\ ^3D_2$
79 649.5	88 888.1*	$^1D_2$		100	0	$(^2D^o)5p\ ^1F_3$
79 668.7	88 907.3*	$^1D_2$		45	55	$(^2D^o)5p\ ^3D_3$
79 683.5	88 922.1	$^1D_2$	88 925[d]	-	-	$(^2P^o)4p\ ^1P_1$
81 882.7	91 121.3	$^1D_2$	91 123[c]	3	97	$(^2P^o)4p\ ^1S_0$
87 227.3	87 623.4	$^3P_1$	87 624[b]	20	80	$(^2P^o)4p\ ^1P_1$
87 414.2	87 810.3*	$^3P_1$		11	89	$(^2P^o)4p\ ^3S_1$
87 624.1	87 624.1	$^3P_2$	87 624[b]	12	88	$(^2P^o)4p\ ^1P_1$
87 810.5	87 810.5*	$^3P_2$		23	77	$(^2P^o)4p\ ^3S_1$
88 303.1	88 876.7	$^3P_0$	88 876[d]	62	38	$(^2D^o)5p\ ^3D_2$
88 466.2	88 862.3*	$^3P_1$		74	26	$(^2D^o)5p\ ^3D_1$
88 481.2	88 877.3	$^3P_1$	88 876[d]	64	36	$(^2D^o)5p\ ^3D_2$
88 492.2	88 888.3*	$^3P_1$		100	0	$(^2D^o)5p\ ^1F_3$
88 510.6	88 906.7*	$^3P_1$		71	29	$(^2D^o)5p\ ^3D_3$
88 526.5	88 922.6	$^3P_1$	88 925[d]	13	87	$(^2P^o)4p\ ^1D_2$
88 861.6	88 861.6*	$^3P_2$		76	24	$(^2D^o)5p\ ^3D_1$
88 877.2	88 877.2	$^3P_2$	88 876[d]	71	29	$(^2D^o)5p\ ^3D_2$
88 906.3	88 906.3*	$^3P_2$		77	23	$(^2D^o)5p\ ^3D_2$
88 922.7	88 922.7	$^3P_2$	88 925[d]	13	87	$(^2P^o)4p\ ^1D_2$

[a]Excited state energy calculated with respect to the $^3P_2$ ground state.
[b]Excited state energy previously reported by Appling *et al.* (Ref. 10).
[c]Excited state energy previously reported by Ventikachalam *et al.* (Ref. 9).
[d]Excited state energy previously reported by Steadman and Baer (Ref. 7).

depend on the laser power, the $^4S^o$ branching ratio diminishing as the laser power increases. This power dependence is indeed observed, as can be seen in Figs. 3(a) and (b), which show photoelectron spectra recorded for ionization *via* the $(^2P^o)4p\ ^3D_1$ level at a two-photon energy of 87 829.7 cm^{-1} (see Table I), employing low laser power in (a) and high laser power in (b). Although comparison of the peak heights in Figs. 3(a) and (b) is not allowed, as the peaks in Fig. 3(b) are broadened by space charge effects, careful

determination of the integrated intensities shows that in Fig. 3(b) the $^2P^o$ and $^2D^o$ branching ratios are indeed significantly larger than in Fig. 3(a), whereas the $^2P^o$:$^2D^o$ ratio stays the same, as expected. A similar power dependence of ionic state branching ratios has been reported previously for $(2+1)$ REMPI *via* autoionizing states of atomic oxygen.[22]

The ionic state branching ratios for ionization *via* the $(^2P^o)4p\ ^3D_J$ states show a strong J dependence. An example is shown in Fig. 4, where the photoelectron spectra for
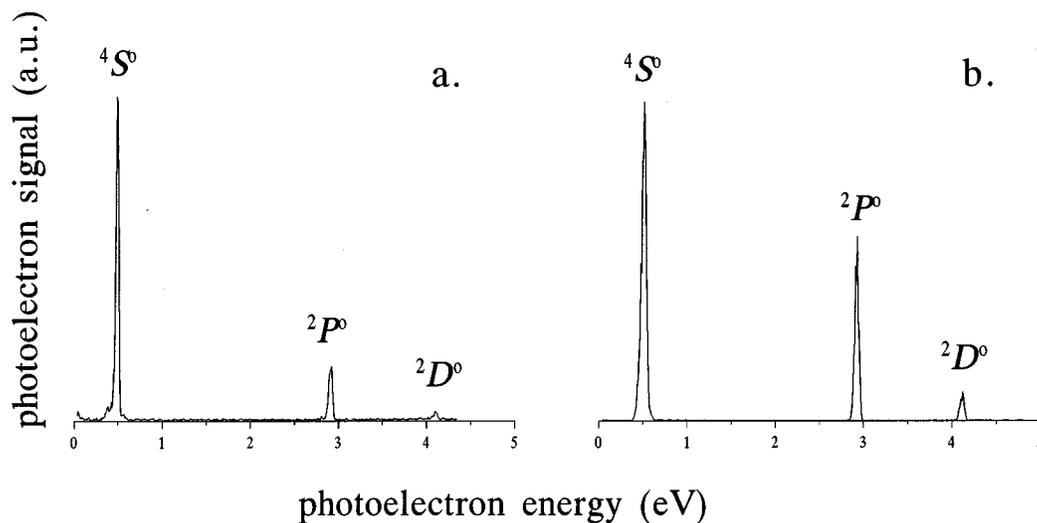

FIG. 3. Photoelectron spectra following excitation of the $(^2P^o)4p\ ^3D_1$ state employing low (a) and high (b) laser intensities.
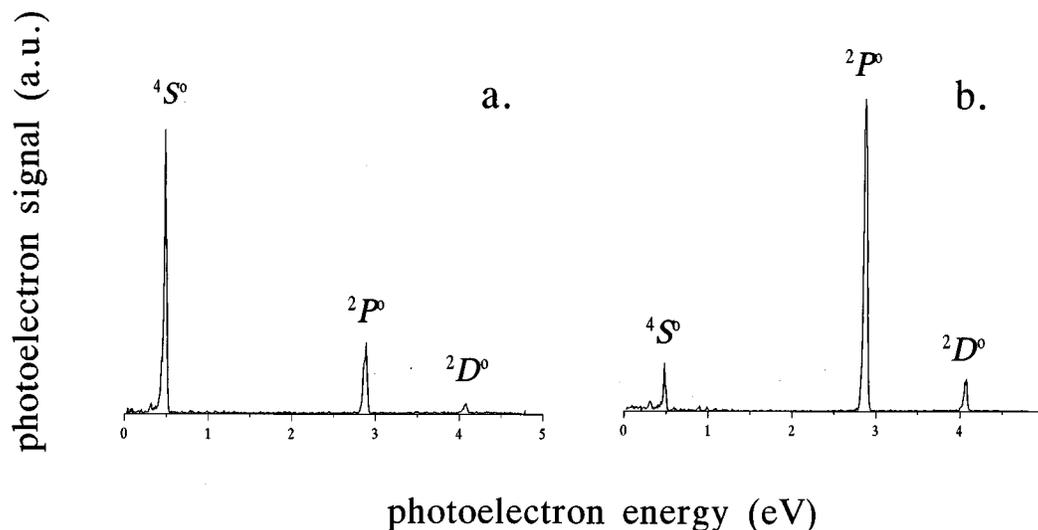
FIG. 4. Photoelectron spectra observed following excitation of the $(^2P^o)4p\ ^3D_1$ (a) and $(^2P^o)4p\ ^3D_3$ (b) fine-structure states.

ionization *via* the $^3D_1$ and $^3D_3$ components are displayed, recorded with equal laser intensities at two-photon energies of 87 433.6 and 87 440.2 cm^{-1}, respectively (see also Table I). Ionization *via* the $^3D_1$ and $^3D_2$ components is observed to produce mainly $^4S^o$ ions, whereas ionization *via* the $^3D_3$ component produces only 10% $^4S^o$ ions and 80% $^2P^o$ ions, providing an interesting example of state-selective photoionization. Under the assumption that the photoionization cross section is independent of J, this would imply that the autoionization rate for the $^3D_3$ component is at least an order of magnitude smaller than for the other two components. This effect can be understood on the basis of the autoionization selection rules.[23] As there are no even-parity ^3D continua associated with the $^4S^o$ core, the ^3D state cannot autoionize electrostatically and must autoionize entirely through spin interactions, possibly spin–orbit coupling. The selection rules for such a coupling would allow for the interaction with several $^4S^o$ ionization continua. The observation that the $(^2P^o)4p\ ^3D_3$ state, however, has a considerably smaller autoionization rate than the $(^2P^o)4p\ ^3D_1$ and $^3D_2$ states, suggests that the dominant interaction concerns spin–orbit coupling with the $(^4S^o)\epsilon p\ ^3P$ continua. As the ^3P continua have no $J=3$ component, and since autoionization can only occur with $\Delta J=0$, only the $^3D_1$ and $^3D_2$ states can autoionize into these continua, while the $^3D_3$ state is expected to remain unaffected.

All the photoelectron spectra for ionization *via* the $(^2P^o)4p\ ^3D$ levels show a small peak corresponding to the production of S$^+(^2D^o)$. This is probably due to configuration interaction of these states with the $(^2D^o)5p\ ^3D$ state (see Sec. C).

The photoelectron spectra for ionization *via* the $(^2D^o)5p\ ^3F$ states show only transitions to the $^2D^o$ and $^4S^o$ ionic states, the latter being accessed by autoionization. The $^4S^o$ branching ratio depends weakly on the J quantum number, being larger for $^3F_2$ than for $^3F_3$ and $^3F_4$. This suggests that the autoionization process proceeds partly

through spin–spin interactions with the $(^4S^o)\epsilon p\ ^3P$ continua, which can affect the $^3F_2$ component, but not the $^3F_3$ and $^3F_4$ components. However, as the $^4S^o$ branching ratios are still appreciable for the $^3F_3$ and $^3F_4$ components, the most important autoionization channel is probably electrostatic interaction with the $(^4S^o)\epsilon f\ ^3F$ continua.

C. Other $(^2P^o)4p$ and $(^2D^o)5p$ states in the energy region 87 000–89 000 cm^{-1}

In addition to the transitions discussed above, many other resonances can be seen in Fig. 1, corresponding to transitions from the ^3P ground state to energy levels in the region from 87 000 to 89 000 cm^{-1}. Most of these resonances are weak. Also, transitions from the $^1D_2$ state to some of these excited states are observed at two-photon energies of about 80 000 cm^{-1}. The transitions from the $^1D_2$ state can easily be recognized as such by their photoelectron spectra.[7] The line positions of the transitions are given in Table III. Some of the energy levels have been reported previously, accessed from either the $^1D_2$ or $^1S_0$ excited state. When this is the case, the reported energy is also given in the table. Photoelectron spectra have been recorded for all but one of the transitions. In general, these spectra show a peak deriving from autoionization into the $^4S^o$ continua and $(2+1)$ ionization into the $^2D^o$ and $^2P^o$ continua. Since in this section we are primarily interested in the identification of states responsible for the resonance enhancement in the excitation spectra, and since the branching ratio to the $^4S^o$ autoionization continua is dependent on the intensity of the excitation laser, Table III only contains such ratios for the $^2D^o$ and $^2P^o$ ionic states.

In Table III tentative assignments are given, which are based on the relative intensities of the transitions and the observed ionic state branching ratios. As has been mentioned above, the excited states in this energy region are expected to have either a $(^2D^o)5p$ or a $(^2P^o)4p$ configuration. Since ionization of a Rydberg state should in principle occur with

core preservation, the photoelectron spectra should give an unambiguous identification of the ionic core. However, $(^2D^o)5p$ and $(^2P^o)4p$ states having the same angular momentum composition (L,S,J) are likely to show substantial configuration interaction. Furthermore, the photoionization matrix elements may differ considerably for different cores, and a strong peak in the photoelectron spectrum may well be due to a minor contribution in the wave function. This makes the assignment a delicate matter. In what follows, each of the tentative assignments given in Table III will be discussed separately.

The state at 87 624 cm^{-1} has been reported previously[10] and has been assigned as $(^2D^o)5p\ ^1P_1$. The fact that no transition from the $^3P_0$ level to this state was observed in the present study, and that no transitions from the $^1S_0$ state have occurred in previous two-photon excitation studies,[7] confirms the assignment of this state as $^1P_1$. However, the photoelectron spectra recorded at two-photon energies of 87 624.1 and 78 385.6 cm^{-1} both show a $^2D^o$:$^2P^o$ ratio of 1:7, which suggests that the configuration is $(^2P^o)4p$ rather than $(^2D^o)5p$. In Ref. 10, a photoelectron spectrum has also been recorded, which only showed S$^+(^4S^o)$, probably because of the lower laser powers employed in the experiment. Accordingly, the state is reassigned here as $(^2P^o)4p\ ^1P_1$.

The state at 88 878 cm^{-1} has been reported previously[7] at an energy of 88 876$\pm$2 cm^{-1}, and has been assigned as $(^2P^o)4p\ ^3P$. This is rather unlikely, since the ^3P state is expected to be strongly autoionizing, and no S$^+(^4S^o)$ was observed in the photoelectron spectrum.[7] Here, an alternative assignment is proposed. The fact that the excited state is observed to be accessible from the $^3P_2$, $^3P_1$, and $^3P_0$ levels implies that it must have a total angular momentum $J=2$ ($J=0\leftrightarrow J=1$, two-photon transitions are strictly forbidden). Furthermore, the transition from the $^1D_2$ level to the excited state is very weak compared to other transitions from the $^1D_2$ level in the same energy region, suggesting that the excited state is a triplet level. For reasons already mentioned, it is unlikely that it is a $(^2D^o)5p\ ^3P_2$ or a $(^2P^o)4p\ ^3P_2$ level. The $(^2D^o)5p\ ^3F_2$ and $(^2P^o)4p\ ^3D_2$ levels have already been assigned (see previous section), and the only remaining triplet state with $J=2$ is therefore $(^2D^o)5p\ ^3D_2$. For this reason the excited state is reassigned as $(^2D^o)5p\ ^3D_2$. Note that this assignment is supported by the photoelectron spectrum.

A consequence of such an assignment is that the $(^2D^o)5p\ ^3D$ state would lie above the $(^2D^o)5p\ ^3F$ state, whereas for the $(^2P^o)4p\ ^3F$ and $(^2D^o)4p\ ^3D$ states the ordering has been found to be reversed. An explanation for this effect might be configuration interaction between the $(^2D^o)5p\ ^3D$ and $(^2P^o)4p\ ^3D$ states, causing the $(^2D^o)5p\ ^3D$ level to shift towards higher energy, while the $(^2D^o)5p\ ^3F$ state remains unaffected, as there is no ^3F state associated with the $(^2P^o)4p$ configuration. Such a configuration interaction nicely explains the $^2P^o$:$^2D^o$ branching ratio of 1:2 observed for ionization of the presumed $(^2D^o)5p\ ^3D_2$ state. In the previous section it was observed that all the photoelectron spectra obtained for $(2+1)$ ionization of the $(^2P^o)4p\ ^3D_2$ level showed contributions of ion-
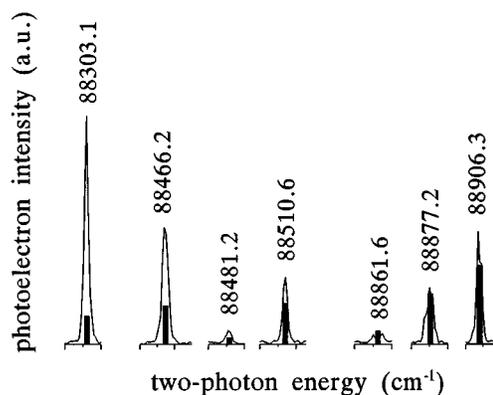

FIG. 5. Detailed wavelength scans showing some of the transitions listed in Table III. The scans were recorded employing kinetic-energy resolved electron detection, monitoring electrons with kinetic energies >2.5 eV. All scans were recorded with equal laser intensity. The bars represent calculated two-photon line strengths for $^3P\rightarrow^3D$ fine-structure transitions (see the text for details).

ization to the $^2D^o$ ionic state. This can now be understood, as the effects of configuration interaction between the $(^2D^o)5p\ ^3D_2$ and the $(^2P^o)4p\ ^3D_2$ levels will similarly be visible in the photoelectron spectra of the latter level. The present assignment leads to the conclusion that the $^3P\rightarrow(^2D^o)5p\ ^3D$ transitions are much weaker than the $^3P\rightarrow(^2D^o)5p\ ^3F$ transitions, implying that for the latter the absolute two-photon absorption cross sections are significantly larger. At present no calculations of these cross sections are available, but *ab initio* calculations on oxygen[24] have shown that for this atom the two-photon absorption cross sections for $^3P\rightarrow(^2D^o)3p\ ^3D$ are indeed five times smaller than for $^3P\rightarrow(^2D^o)3p\ ^3F$.

The other two components of the ^3D triplet may be expected to lie near the $(^2D^o)5p\ ^3D_2$ state. For the $(^2D^o)5p\ ^3D$ state the splittings are expected to be smaller by a factor $(\frac{4}{5})^3\approx0.5$ as compared to the $4p$ series member. It therefore appears that the term levels at 88 906.3 and 88 861.6 cm^{-1}, the photoelectron spectra of which show $^2P^o$:$^2D^o$ branching ratios of ~1:3, might be the $^3D_1$ and $^3D_3$ components. This assumption is supported by the observation that neither of these states is accessed from the $^3P_0$ level. Detailed wavelength scans employing kinetic energy-resolved electron detection were recorded in order to obtain accurate estimates for the relative intensities of the transitions from the $^3P_1$ and $^3P_2$ levels to these states (see Fig. 5). Comparison of the theoretical values for the relative line strengths for a $^3P\rightarrow^3D$ transition[21] and the observed intensities suggests that the level at 88 861.6 cm^{-1} might be assigned as $^3D_1$ and the level at 88 906.3 cm^{-1} as $^3D_3$.

A strong transition from the $^1D_2$ state is observed at a two-photon energy of 79 649.5 cm^{-1}, corresponding to an energy of 88 888.1 cm^{-1} for the excited state. No transitions from the $^3P_2$ or $^3P_0$ ground-state levels to this excited state are observed, but a weak transition at a two-photon energy of 88 492.2 cm^{-1}, which has no $^3P_2$ or $^3P_0$ counterparts, is tentatively assigned as a transition from the $^3P_1$ level to this

excited state. The state is likely to be a singlet, since the transition from the $^1D_2$ state is very strong and the transition from the $^3P_1$ state is rather weak. The photoelectron spectra show that $(2+1)$ ionization occurs exclusively to the $^2D^o$ ionic state, implying that the configuration is $(^2D^o)5p$ and that the state possesses no $(^2P^o)4p$ character whatsoever. The possible $(^2D^o)5p$ singlet states are $^1P_1$, $^1D_2$, and $^1F_3$. $^1P_1$ and $^1D_2$ states can also arise from the $(^2P^o)4p$ configuration, which implies that if the excited state were either $(^2D^o)5p$ $^1P_1$ or $(^2D^o)5p$ $^1D_2$, at least some $(^2P^o)4p$ character would be expected to mix in and show up in the photoelectron spectra. Therefore, the state is assigned as $(^2D^o)5p$ $^1F_3$. This assignment implies that the $^1F_3 - {}^3F_3$ splitting has decreased by a factor $88/200 \approx 0.44$ compared to the previous series member, which is indeed of the order of the expected factor $(\frac{4}{5})^3 \approx 0.5$.

At two-photon energies of 87 414.2 and 87 810 cm^{-1}, two peaks are observed that correspond to transitions from the $^3P_1$ and $^3P_2$ levels to a state at 87 811.5 cm^{-1}. The fact that a transition from the $^3P_0$ level is not observed suggests that the excited state has either $J=1$ or $J=3$. No transition from the $^1D_2$ level to this state is observed either, suggesting that it is a triplet state. Inspection of the photoelectron spectra obtained after excitation of this state shows that ionization occurs preferentially to the $^2P^o$ ionic state. If we assume that this state is indeed built upon the $^2P^o$ ionic core, we have to conclude that its assignment is $(^2P^o)4p$ $^3S_1$. Such an assignment is supported by the observation that the state seems to have only a single level, but would violate the LS-coupling selection rule that $L=0 \leftrightarrow L=1$ transitions are forbidden. This would imply that for this state LS-coupling is not strictly valid. The fact that a significant ionization to the $^2D^o$ ionic state is observed indicates that the $^3S_1$ state is coupled to a state with a $^2D^o$ ionic core and $J=1$, from which it obtains transition probability.

The resonance at 81 882.7 cm^{-1} corresponds to a transition from the $^1D_2$ state to a state at 91 121 cm^{-1}, which has been reported previously[7,25] and assigned as $(^2P^o)4p$ $^1S_0$. Since the photoelectron spectrum recorded at 81 882.7 cm^{-1} shows a $^2P^o:{}^2D^o$ branching ratio of 30:1, this assignment was assumed in Table III. As the $(^2P^o)4p$ $^1P_1$ and $(^2P^o)4p$ $^1S_0$ states have now both been assigned, the only $(^2P^o)4p$ singlet state left to be found is $(^2P^o)4p$ $^1D_2$. The state at 87 810 cm^{-1} can be excluded, as it is observed not to be accessible from the $^1D_2$ state. The only remaining observed state with a high $^2P^o$ branching

ratio is the state at 88 923 cm^{-1}, which shows a $^2P^o:{}^2D^o$ branching ratio of 7:1. A strong transition at 79 683.5 cm^{-1} from the $^1D_2$ state to this level suggests that it is in effect a singlet state. Accordingly, it is assigned as $(^2P^o)4p$ $^1D_2$. As has already been mentioned in the previous section, a transition from the $^1S_0$ state to this level has been observed, and assigned as $(^2P^o)4p$ $^3D_2$.[7] However, the present study shows that the $(^2P^o)4p$ ^3D state lies at a much lower energy.

ACKNOWLEDGMENTS

[1] Z. Altun, J. Phys. B **25**, 2279 (1992).
[2] R. P. Wayne, J. Photochem. Photobiol. A-Chemistry **62**, 379 (1992).
[3] G. Tondello, Astrophys. J. **172**, 771 (1972).
[4] V. N. Sarma and Y. N. Joshi, Physica C **123**, 349 (1984).
[5] Y. N. Joshi, M. Mazzoni, A. Nenecioni, W. H. Parkinson, and A. Cantu, J. Phys. B **20**, 1203 (1987).
[6] S. T. Gibson, J. P. Greene, B. Ruscić, and J. Berkowitz, J. Phys. B **19**, 2825 (1986).
[7] J. Steadman and T. Baer, J. Chem. Phys. **89**, 5507 (1988).
[8] P. Brewer, N. van Veen, and R. Bersohn, Chem. Phys. Lett. **91**, 126 (1982).
[9] T. V. Ventikachalam and A. S. Rao, Appl. Phys. B **52**, 102 (1991).
[10] J. R. Appling, M. R. Harbol, and R. A. Edgington, J. Chem. Phys. **97**, 4041 (1992).
[11] S. T. Pratt, Phys. Rev. A **38**, 1270 (1988).
[12] S. Woutersen, J. B. Milan, W. J. Buma, and C. A. de Lange, Phys. Rev. A **54**, 5126 (1996).
[13] E. de Beer, C. A. de Lange, and N. P. C. Westwood, Phys. Rev. A **46**, 5653 (1992).
[14] B. G. Koenders, D. M. Wieringa, K. E. Drabe, and C. A. de Lange, Chem. Phys. **118**, 113 (1987).
[15] C.-W. Hsu, C. L. Liao, Z.-X. Ma, P. J. H. Tjossem, and C. Y. Ng, Chem. Phys. Lett. **199**, 78 (1992).
[16] W. C. Martin, R. Zalubas, and A. Musgrove, J. Phys. Chem. Ref. Data **19**, 820 (1990).
[17] A. V. Smith, T. D. Raymond, and M. E. Riley, Phys. Rev. A **45**, 4688 (1992).
[18] G. Grynberg, F. Biraben, E. Giacobino, and B. Cagnac, J. Phys. (Paris) **38**, 629 (1977).
[19] B. Cagnac, G. Grynberg, and F. Biraben, J. Phys. (Paris) **34**, 845 (1973).
[20] I. Sobelman, *Atomic Spectra and Radiative Transitions* (Springer Verlag, New York, 1979).
[21] P. Das, G. Ondrey, N. van Veen, and R. Bersohn, J. Chem. Phys. **79**, 724 (1983).
[22] S. T. Pratt, P. M. Dehmer, and J. L. Dehmer, Phys. Rev. A **43**, 282 (1991).
[23] P. Feldman and R. Novick, Phys. Rev. **160**, 143 (1967).
[24] R. P. Saxton and J. Eichler, Phys. Rev. A **34**, 199 (1986).
[25] M. Kawasaki, H. Sato, Kobayashi, and T. Arikawa, Chem. Phys. Lett. **146**, 101 (1988).